

1 **Nitrogen Isotope Simulations Confirm the Importance of Atmospheric Iron**
2 **Deposition for Nitrogen Fixation Across the Pacific Ocean**

3
4 Christopher J. Somes^{1*}, Andreas Schmittner¹, and Mark A. Altabet²

5
6 ¹ *College of Oceanic and Atmospheric Sciences, Oregon State University, Corvallis, Oregon,*
7 *USA*

8
9 ² *School for Marine Science and Technology, U. Massachusetts Dartmouth, New Bedford,*
10 *Massachusetts, USA*

11
12 * Author to whom correspondence should be addressed (email: csomes@coas.oregonstate.edu)

Abstract

Nitrogen (N) fixation by specialized microorganisms (diazotrophs) influences global plankton productivity because it provides the ocean with most of its bio-available N. However, its global rate and large-scale spatial distribution is still regarded with considerable uncertainty. Here we use a global ocean nitrogen isotope model, in comparison with $\delta^{15}\text{NO}_3^-$ observations, to constrain the pattern of N_2 fixation across the Pacific Ocean. N_2 fixation introduces isotopically light atmospheric N_2 from the ocean ($\delta^{15}\text{N} = 0\text{‰}$) relative to the oceanic average near 5‰, which makes nitrogen isotopes suitable to infer patterns of N_2 fixation. Including atmospheric iron limitation of diazotrophy in the model shifts the pattern of simulated N_2 fixation from the South Pacific to the North Pacific and from the East Pacific westward. These changes considerably improve the agreement with meridional transects of available $\delta^{15}\text{NO}_3^-$ observations, as well as excess P ($\text{PO}_4^{3-} - \text{NO}_3^-/16$), confirming that atmospheric iron deposition is indeed important for N fixation in the Pacific Ocean. This study highlights the potential for using $\delta^{15}\text{N}$ observations and model simulations to constrain patterns and rates of N fixation in the ocean.

1. Introduction

Nitrogen (N) fixation is regarded as the dominant source of biologically available nitrogen (fixed-N) into the ocean [Codispoti, 2007], which is performed by specialized prokaryotes (diazotrophs) that are capable of reducing N_2 gas instead of forms of oceanic fixed-N (NO_3^- , NO_2^- , NH_4^+) during photosynthesis. Since diazotrophs are not limited by fixed-N, they can grow in N-depleted surface water provided other required nutrients (e.g., phosphorus (P) and iron (Fe)) are available for uptake. Diazotrophs can have an important influence on climate because fixed-N limits primary production and biological sequestration of atmospheric CO_2 . The large spatial and temporal variability of diazotrophs makes it difficult to constrain the global rate of N_2 fixation. Recent estimates of N_2 fixation have seen upward revisions, but still range widely between $\sim 100 - 200 \text{ Tg N yr}^{-1}$ [Gruber and Sarmiento, 1997; Karl et al., 2002; Deutsch et al., 2007; Moore and Doney, 2007]. The efficiency, with which diazotrophs can balance the N-loss from denitrification and anammox, the major sinks for fixed-N, largely determines if the oceanic fixed-N inventory could fluctuate significantly enough to affect atmospheric CO_2 through changes in the biological pump.

Throughout much of the contemporary ocean, biological productivity is limited by fixed-N suggesting other factors are preventing diazotrophs from fixing N, such as light, temperature, and/or P and Fe availability. It follows that blooms of *Trichodesmium*, one of the most important and best studied diazotrophs, occur more frequently and are more extensive in warm ($>25^\circ\text{C}$) surface water where rates of atmospheric Fe deposition are high such as the North Atlantic, Indian, and North Pacific compared to areas of low Fe deposition such as the South Pacific where the abundance of *Trichodesmium* appears to be much lower [Carpenter, 1983; Karl et al., 2002; Carpenter and Capone, 2008]. This suggests that temperature and Fe availability may be

the most important factors that determine where N_2 fixation is able to occur. However, other more uncharacterized unicellular diazotrophs have been observed to grow in cooler water near 20°C [Needoba *et al.*, 2007], and it has been suggested that they also may significantly contribute to the global N_2 fixation rate [Zehr *et al.*, 2001; Montoya *et al.*, 2004].

N_2 fixation introduces relatively isotopically light N ($\delta^{15}\text{N} = 0\text{‰}$) into the ocean compared to the global mean $\delta^{15}\text{NO}_3^-$ near 5‰. Therefore, the ratio of the two stable nitrogen isotopes, represented in the $\delta^{15}\text{N}$ notation where $\delta^{15}\text{N} = [({}^{15}\text{N}/{}^{14}\text{N})_{\text{sample}}/({}^{15}\text{N}/{}^{14}\text{N})_{\text{atmosphere}} - 1] \cdot 1000$, may be a powerful tool to trace patterns of N_2 fixation. We will compare a model of nitrogen isotopes, embedded within the ocean component of a global Earth System Climate Model, with $\delta^{15}\text{NO}_3^-$ measurements across the Pacific Ocean to constrain N_2 fixation. We focus on the effect of atmospheric Fe limitation of diazotrophy.

2. Model Description

2.1 Marine Ecosystem/Biogeochemical Model

The marine ecosystem/biogeochemical model is the NPZD (Nutrient, Phytoplankton, Zooplankton, Detritus) ecosystem model of *Somes et al.*, [2010]. The organic variables include two classes of phytoplankton, diazotrophs (P_D), which can undergo N_2 fixation (Figure 1), and a “general” NO_3^- assimilating phytoplankton class (P_G), as well as zooplankton (Z) and organic detritus (D). The inorganic variables include dissolved oxygen (O_2) and two nutrients, nitrate (NO_3^-) and phosphate (PO_4^{3-}), both of which are consumed by phytoplankton and remineralized in fixed elemental ratios ($R_{N:P} = 16$, $R_{O:P} = 170$). We note, though, that diazotrophs have been found to have $R_{N:P}$ as high as 50:1 (e.g., *Letelier and Karl*, [1996; 1998]). This simplification is one of the reasons why excess phosphorus, $\text{xsP} = \text{PO}_4^{3-} - \text{NO}_3^-/16$, is generally overestimated near the surface in the model (Figure 2). Denitrification, the replacement of O_2 with NO_3^- as the

electron acceptor during the respiration of organic matter, occurs under suboxic conditions ($O_2 < 5 \mu M$) in the water column and the sea floor sediments [Codispoti and Richards, 1976]. Since the model underestimates coastal upwelling (due to its coarse resolution), which drives large fluxes of organic carbon to the sea floor that create suboxic conditions in the sediments, the benthic denitrification parameterization [Middleburg *et al.*, 1996] is tuned to set the global mean $\delta^{15}NO_3^-$ to observations near 5‰ by multiplying this parameterization by a constant factor ($\alpha_{SD} = 8$) (see *Somes et al.*, [2010]).

Diazotrophs grow according to the same principles as general phytoplankton in the model, but we also account for some of their different characteristics. N_2 fixation breaks down the triple-N bond of N_2 , which is energetically more costly than assimilating fixed-N. Therefore, in the model, the growth rate of diazotrophs is lower than that of general phytoplankton. It is zero in waters cooler than $15^\circ C$ and increases 40% slower with temperature than the growth rate of general phytoplankton. Diazotrophs are not limited by NO_3^- and can out-compete general phytoplankton in surface waters that are depleted in fixed-N, but still contain sufficient P (i.e., high xsP water due to denitrification). However, diazotrophs will consume NO_3^- if it is available, consistent with culture experiments [Mulholland *et al.*, 2001; Holl and Montoya, 2005], which is another factor that inhibits N_2 fixation in the model. Denitrification, and the propagation of N-deficient waters into the shallow thermocline by physical transport processes, creates an ecological niche for diazotrophs in the model, which stimulates N_2 fixation [Tyrrell, 1999]. Fe is currently not included as a prognostic tracer in the model. However, we include a simple parameterization of atmospheric Fe limitation of diazotrophy as described in Section 3.

2.2 Nitrogen Isotope Model

The nitrogen isotope model simulates the distribution of the two stable nitrogen isotopes, ^{14}N and ^{15}N , in all N species included in the marine ecosystem model. The processes in the model that fractionate nitrogen isotopes are algal NO_3^- assimilation ($\epsilon_{\text{ASSIM}} = 5\text{‰}$), zooplankton excretion ($\epsilon_{\text{EXCR}} = 6\text{‰}$), water column denitrification ($\epsilon_{\text{WCD}} = 25\text{‰}$), and N_2 fixation ($\epsilon_{\text{NFIX}} = 1.5\text{‰}$). Fractionation results in the isotopic enrichment of the more reactive, thermodynamically preferred, light ^{14}N into the product of each reaction by a process-specific fractionation factor. For a detailed discussion of nitrogen isotope fractionation dynamics see [Mariotti *et al.*, 1981]. Although little fractionation occurs during N_2 fixation in the model, it has an important effect on $\delta^{15}\text{N}$ by introducing isotopically light atmospheric N_2 ($\delta^{15}\text{N} = 0\text{‰}$) into the oceanic fixed-N pool. Benthic denitrification has been observed to have little effect on the oceanic isotopic N pool because denitrifiers consume nearly all NO_3^- diffusing into the reactive zones within the sediments, leaving the oceanic N pool mostly unaltered [Brandes and Devol, 2002; Lehmann *et al.*, 2004; Lehmann *et al.*, 2007]. Therefore, in the model, there is no fractionation during benthic denitrification ($\epsilon_{\text{BD}} = 0\text{‰}$), although this is a simplification of observations [Lehmann *et al.*, 2007]. Fractionation during the remineralization of organic matter to NO_3^- is not included in the model. The complete nitrogen isotope model description is provided in *Somes et al.*, [2010].

3. Atmospheric Fe Limitation of Diazotrophy

The nitrogenase enzyme, which fixes N_2 in diazotrophs, has a large structural iron (Fe) requirement [Raven, 1988; Sanudo-Wilhelmy *et al.*, 2001]. Diazotrophs may depend on Fe from atmospheric deposition in oligotrophic waters, where a deep pycnocline inhibits upward mixing of subsurface Fe-replete waters into the euphotic zone. Therefore, we include an atmospheric Fe limitation of diazotrophy experiment (FeLim), where diazotrophs' growth rate is further reduced

by the Fe limitation parameter (FeL), which scales an estimate of monthly climatological atmospheric dust deposition [Mahowald *et al.*, 2005] between 0 and 1 (Figure 1) by multiplying atmospheric dust deposition rate by a constant factor, and setting the maximum value to 1 (i.e., maximum growth rate = $\mu_D \cdot FeL$). We note that the model still does not account for any Fe input from rivers or shelf sediments.

3. Results

The control (CTL) simulation does not include any Fe limitation of diazotrophs (i.e., maximum growth rate = μ_D) and results in large N_2 fixation rates in the Central and Eastern Tropical South Pacific (Figure 1). The only factor that prevents N_2 fixation from occurring in the Eastern Tropical Pacific of CTL is the presence of high surface NO_3^- in the core of the HNLC region, where diazotrophs will consume NO_3^- instead of fixing dissolved N_2 to meet their N requirement for growth. This pattern of tight coupling of N_2 fixation and denitrification in the Eastern Tropical South Pacific is consistent with the model of Deutsch *et al.*, [2007], which predicts N_2 fixation based on the xSP distribution in a general ocean circulation model, but does not include any Fe limitation or NO_3^- inhibition.

Considering atmospheric Fe limitation of diazotrophs (FeLim), the pattern of N_2 fixation—such as high values in the tropical/subtropical North Pacific, the western tropical/subtropical South Pacific, the western tropical/subtropical South Atlantic, the tropical/subtropical North Atlantic and the Indian Ocean—is much more consistent with direct observations (e.g., Karl *et al.*, [2002]; Carpenter and Capone, [2008]), and with results from a more complex ecosystem/biogeochemical model [Moore and Doney, 2007]. However, N_2 fixation in our model does not extend northward of $\sim 30^\circ N$ in the North Pacific, whereas some observations show N_2 fixation as far north as $35\text{--}40^\circ N$ [Church *et al.*, 2008; Kitajima *et al.*, 2009]. We hypothesize

this discrepancy occurs due to the oversimplified fast-recycling microbial loop parameterization, which recycles organic matter to inorganic nutrients at N:P=16. It has been suggested that P recycles more efficiently relative to N through these microbial loops [Wu *et al.*, 2000], which is a mechanism that could help relieve diazotrophs of their P limitation throughout the tropical/subtropical oligotrophic ocean and stimulate additional N₂ fixation.

Global measures of $\delta^{15}\text{NO}_3^-$ and xsP improve in FeLim compared to CTL (Table 1). Generally lower $\delta^{15}\text{NO}_3^-$ and xsP in the Northern Hemisphere relative to the Southern Hemisphere in FeLim, due to more N₂ fixation occurring in the Northern Hemisphere where more atmospheric Fe deposition exists, result in a better match with observations than in CTL (Figure 2). The Central and Western Tropical Pacific are both “downstream” from the suboxic zones in the Eastern Pacific, representing potential regions where N₂ fixation may occur as high xsP flows westward out of the Eastern Pacific denitrification zones. Measured $\delta^{15}\text{NO}_3^-$ shows a decreasing trend northwards in the two transects across the Pacific (Figure 3), with a minimum near the equator in the Central Pacific transect. This equatorial minimum is reproduced in the model due to the low degree of surface NO_3^- utilization as a result of extensive NO_3^- supply to the surface from equatorial upwelling. The northward decreasing $\delta^{15}\text{NO}_3^-$ trend in FeLim in both transects is due to more N₂ fixation occurring north of the equator, where sufficient atmospheric Fe deposition exists (Figure 1). When atmospheric Fe limitation of diazotrophy is not included in the model (CTL), the opposite $\delta^{15}\text{NO}_3^-$ trend is simulated because more N₂ fixation occurs south of the equator, in contrast to the observations.

4. Discussion

We have highlighted two affects that can prevent N₂ fixation in the Pacific: Fe limitation and NO₃⁻ inhibition. Nitrate contours in World Ocean Atlas 2005 (WOA) show the potential effect of NO₃⁻ inhibition on N₂ fixation. xsP is generally not restored close to 0 (~0.1 - 0.2 μM) until near-surface (0 – 100 m) NO₃⁻ is almost completely consumed in the Western Pacific (see 0.5 μM NO₃⁻ contour, Figure 2), but xsP remains high (> ~0.4 μM) where large near-surface NO₃⁻ concentrations exist in the Eastern Pacific (see 5.0 μM NO₃⁻ contour, Figure 2). A meridional gradient in the Western Tropical Pacific appears in the observations such that xsP in South Pacific remains mostly above ~0.1 μM, whereas it is lower than 0.1 μM in the North Pacific. This suggests that Fe is preventing N₂ fixation in the South Pacific but not in the North Pacific, where atmospheric Fe deposition is much higher. The high xsP water that flows out of the ETSP denitrification zone into the Southern Ocean may remain high in xsP until it reaches a region with sufficient Fe (e.g., North Atlantic or North Indian Ocean), which could take several hundreds of years, and result in a significant decoupling of N₂ fixation from denitrification that occurs in the Fe-depleted Southern Hemisphere (see also *Falkowski [1997]*).

4. Conclusion

Model simulations that include Fe limitation of diazotrophy show a much better agreement with δ¹⁵NO₃⁻ and xsP observations compared to a model that neglects this effect (Table 2, Figures 2, 3). Nitrate isotope observations show a decreasing northward trend across two transects in the Central and Western Pacific (Figure 3). Comparisons with model results reveal that these trends can be best explained by the input of isotopically light N by N₂ fixation, where higher rates of atmospheric Fe deposition exist. This highlights the potential of δ¹⁵NO₃⁻ as a tool to infer the spatial pattern of N₂ fixation. If no N₂ fixation was occurring, the δ¹⁵NO₃⁻

187 value would be expected to be very high ($\delta^{15}\text{NO}_3^- > 10\text{‰}$) due to the nearly complete utilization
188 of surface NO_3^- in the oligotrophic ocean [Altabet and Francois, 1994; Somes *et al.*, 2010],
189 which is a drastically different $\delta^{15}\text{N}$ signature than what would be expected if N_2 fixation was
190 significantly contributing to the local N pool ($\delta^{15}\text{N}_2 = 0\text{‰}$). Our results suggest that $\delta^{15}\text{N}$
191 observations, in combination with models, can be used to constrain N_2 fixation patterns in
192 present and past oceans.

193

194 **Acknowledgements**

195 Thanks to Eric Galbraith, Moritz Lehman, Joseph Montoya, Ricardo Letelier, and Alan Mix for
196 helpful comments. This work is funded by the Marine Geology and Geophysics program of the
197 National Science Foundation (0728315-OCE).

198

References Cited

- Altabet, M. A. (2001), Nitrogen isotopic evidence for micronutrient control of fractional NO₃ utilization in the equatorial Pacific, *Limnology and Oceanography*, 46(2), 368-380.
- Altabet, M. A., and R. Francois (1994), Sedimentary nitrogen isotopic ratio as a recorder for surface ocean nitrate utilization, *Global Biogeochem. Cycles*, 8(1), 103-116, doi:10.1029/93GB03396.
- Brandes, J. A., and A. H. Devol (2002), A global marine-fixed nitrogen isotopic budget: Implications for Holocene nitrogen cycling, *Global Biogeochem. Cycles*, 16(4), 1120, doi:10.1029/2001GB001856.
- Carpenter, E. J. (1983), Nitrogen fixation by marine Oscillatoria (*Trichodesmium*) in the world's oceans, in *Nitrogen in the Marine Environment*, edited by E. J. Carpenter and D. G. Capone, pp. 65-103, Academic, San Diego, California.
- Carpenter, E. J., and D. G. Capone (2008), Nitrogen Fixation in the Marine Environment, in *Nitrogen in the Marine Environment*, edited by D. G. Capone, D. A. Bronk, M. R. Mulholland and E. J. Carpenter, pp. 141-198, Elsevier Inc.
- Church, M. J., K. M. Bjorkman, D. M. Karl, M. A. Saito, and J. P. Zehr (2008), Regional distributions of nitrogen-fixing bacteria in the Pacific Ocean, *Limnol. Oceanogr.*, 53(1), 63-77.
- Codispoti, L. A. (2007), An oceanic fixed nitrogen sinke exceeding 400 Tg N a⁻¹ vs the concept of homeostasis in the fixed-nitrogen inventory, *Biogeosciences*, 4, 233-253.

218 Codispoti, L. A., and F. A. Richards (1976), An analysis of the horizontal regime of
 219 denitrification in the eastern tropical North Pacific, *Limnol. Oceanogr.*, *21*(3), 379-388.

220 Deutsch, C., J. L. Sarmiento, D. M. Sigman, N. Gruber, and J. P. Dunne (2007), Spatial coupling
 221 of nitrogen inputs and losses in the ocean, *Nature*, *445*, 163-167, doi: 10.1038/nature05392.

222 Falkowski, P. G. (1997), Evolution of the nitrogen cycle and its influence on the biological
 223 sequestration of CO₂ in the ocean, *Nature*, *387*, 272-275, doi:10.1038/387272a0.

224 Gruber, N., and J. L. Sarmiento (1997), Global patterns of marine nitrogen fixation and
 225 denitrification, *Global Biogeochem. Cycles*, *11*(2), 235, 235-266.

226 Holl, C. M., and J. P. Montoya (2005), Interactions between nitrate uptake and nitrogen fixation
 227 in continuous cultures of the marine diazotroph *Trichodesmium* (cyanobacteria), *J. Phycol.*, *41*,
 228 1178-1183, doi:10.1111/j.1529-8817.2005.00146.x.

229 Karl, D., A. Michaels, B. Bergman, D. Capone, E. Carpenter, R. Letelier, F. Lipshultz, H. Paerl,
 230 D. Sigman, and L. Stal (2002), Dinitrogen fixation in the world's oceans, *Biogeochemistry*,
 231 *57/58*, 47, 47-98.

232 Kienast, M., M. F. Lehmann, A. Timmermann, E. Galbraith, T. Bolliet, A. Holbourn, C.
 233 Normandeau, and C. Laj (2008), A mid-Holocene transition in the nitrogen dynamics of the
 234 western equatorial Pacific: Evidence of a deepening thermocline?, *Geophysical Research Letter*,
 235 *35*, L23610, doi:10.1029/2008GL035464.

236 Kitajima, S., K. Furuya, F. Hashihama, S. Takeda, and J. Kanda (2009), Latitudinal distribution
 237 of diazotrophs and their nitrogen fixation in the tropical and subtropical western North Pacific,
 238 *Limnol. Oceanogr.*, 54(2), 537-547.

239 Lehmann, M. F., D. M. Sigman, and W. M. Berelson (2004), Coupling the $^{15}\text{N}/^{14}\text{N}$ and $^{18}\text{O}/^{16}\text{O}$
 240 of nitrate as a constraint on benthic nitrogen cycling, *Mar. Chem.*, 88, 1-20,
 241 doi:10.1016/j.marchem.2004.02.001.

242 Lehmann, M. F., D. M. Sigman, D. C. McCorkle, J. Granger, S. Hoffmann, G. Cane, and B. G.
 243 Brunelle (2007), The distribution of nitrate $^{15}\text{N}/^{14}\text{N}$ in marine sediments and the impact of
 244 benthic nitrogen loss on the isotopic composition of oceanic nitrate, *Geochim. Cosmochim. Acta*,
 245 71, 5384-5404, doi:10.1016/j.gca.2007.07.025.

246 Letelier, R. M., and D. M. Karl (1996), Role of *Trichodesmium* spp. in the productivity of the
 247 subtropical North Pacific Ocean, *Marine Ecology Progress Series*, 133, 263-273,
 248 doi:10.3354/meps133263, <http://www.int-res.com/abstracts/meps/v133/p263-273/>.

249 Letelier, R. M., and D. M. Karl (1998), *Trichodesmium* spp. physiology and nutrient fluxes in the
 250 North Pacific subtropical gyre, *Aquatic Microbial Ecology*, 15, 254-276,
 251 doi:10.3354/ame015265.

252 Liu, K.-K., M.-J. Su, C.-R. Hsueh, and G.-c. Gong (1996), The nitrogen isotopic composition of
 253 nitrate in the Kuroshio Water northeast of Taiwan: evidence for nitrogen fixation as a source of
 254 isotopically light nitrate, *Marine Chemistry*, 54, 273-292.

255 Mahowald, N. M., A. R. Baker, G. Bergametti, N. Brooks, R. A. Duce, T. D. Jickells, N.
 256 Kubilay, J. M. Prospero, and I. Tegen (2005), Atmospheric global dust cycle and iron inputs to
 257 the ocean, *Global Biogeochem. Cycles*, 19, GB4025, doi:10.1029/2004GB002402.

258 Mariotti, A., J. C. Germon, P. Hubert, P. Kaiser, R. Letolle, A. Tardieux, and P. Tardieux (1981),
 259 Experimental determination of nitrogen kinetic isotope fractionation: some principles;
 260 illustration for the denitrification and nitrification processes, *Plant and Soil*, 62(3), 413-430,
 261 doi:10.1007/BF02374138.

262 Middleburg, J. J., K. Soetaert, P. M. J. Herman, and C. H. R. Heip (1996), Denitrification in
 263 marine sediments: A model study, *Global Biogeochem. Cycles*, 10(4), 661-673,
 264 doi:10.1029/96GB02562

265 Montoya, J. P., C. M. Holl, J. P. Zehr, A. Hansen, T. A. Villareal, and D. G. Capone (2004),
 266 High rates of N₂ fixation by unicellular diazotrophs in the oligotrophic Pacific Ocean, *Nature*,
 267 430, 1027-1031, doi:10.1038/nature02824.

268 Moore, J. K., and S. C. Doney (2007), Iron availability limits the ocean nitrogen inventory
 269 stabilizing feedbacks between marine denitrification and nitrogen fixation, *Global*
 270 *Biogeochemical Cycles*, 21, GB2001, doi: 10.1029/2006GB002762.

271 Mulholland, M. R., K. Ohki, and D. G. Capone (2001), Nutrient controls on nitrogen uptake and
 272 metabolism by natural populations and cultures of *Trichodesmium* (cyanobacteria), *Journal of*
 273 *Phycology*, 37, 1001-1009.

274 Needoba, J. A., R. A. Foster, C. Sakamoto, J. P. Zehr, and K. S. Johnson (2007), Nitrogen
 275 fixation by unicellular diazotrophic cyanobacteria in the temperate oligotrophic North Pacific
 276 Ocean, *Limnol. Oceanogr.*, 52(4), 1317-1327.

277 Raven, J. A. (1988), The iron and molybdenum use efficiencies of plant growth with different
 278 energy, carbon and nitrogen sources, *New Phytologist*, 109(3), 279-287.

279 Sanudo-Wilhelmy, S. A., A. B. Kustka, C. J. Gobler, D. A. Hutchins, M. Yang, K. Lwiza, J.
 280 Burns, D. G. Capone, J. A. Raven, and E. J. Carpenter (2001), Phosphorus limitation of nitrogen
 281 fixation by *Trichodesmium* in the central Atlantic Ocean, *Nature*, 411, 66-69,
 282 doi:10.1038/35075041.

283 Somes, C. J., A. Schmittner, A. C. Mix, R. M. Letelier, E. G. Galbraith, M. F. Lehmann, M. A.
 284 Altabet, J. P. Montoya, M. Eby, and A. Bourbonnais (2010), Simulating the global distribution of
 285 nitrogen isotopes in the ocean, *Global Biogeochem. Cycles*,
 286 http://mgg.coas.oregonstate.edu/~andreas/pdf/S/somes10gbc_subm.pdf.

287 Tyrrell, T. (1999), The relative influences of nitrogen and phosphorus on oceanic primary
 288 production, *Nature*, 400, 525-531, doi:10.1038/22941.

289 Wu, J., W. Sunda, E. A. Boyle, and D. M. Karl (2000), Phosphate depletion in the Western North
 290 Atlantic Ocean, *Science*, 289, 759-762, doi:10.1126/science.289.5480.759.

291 Yoshikawa, C., Y. Yamanaka, and T. Nakatsuka (2006), Nitrate-nitrogen isotopic patterns in
 292 surface waters of the Western and Central Equatorial Pacific, *J. Oceanogr.*, 62, 511-525.

293 Zehr, J. P., J. B. Waterbury, P. J. Turner, J. P. Montoya, E. Omoregie, G. F. Steward, A. Hansen,
294 and D. M. Karl (2001), Unicellular cyanobacteria fix N₂ in the subtropical North Pacific Ocean,
295 *Nature*, 412(9), 635-638, doi:10.1038/35088063.

296

Figure Captions:

Figure 1. Top Panel: Annual rates of dust deposition [Mahowald *et al.*, 2005] and *FeL* parameter used to decrease the growth rate of diazotrophs. Bottom Panel: Vertically integrated N₂ fixation in FeLim and CTL.

Figure 2. Comparison of FeLim and CTL with $\delta^{15}\text{NO}_3^-$ observations [Somes *et al.*, 2010] and World Ocean Atlas 2005: $\text{xsP} = \text{PO}_4^{3-} - \text{NO}_3^-/16$ and near-surface (0 – 100m) NO_3^- contours of 5.0 and 0.5 μM . Note that due to the too low N:P for diazotrophs in the model (N:P = 16:1) compared to observations (N:P = ~50:1) [Letelier and Karl, 1996; 1998], a slight overestimation of xsP is to be expected where N₂ fixation occurs.

Figure 3. Comparison of FeLim and CTL $\delta^{15}\text{NO}_3^-$ with observations in the (a) Central Equatorial Pacific (140°W) (100 – 250 m) [Altabet, 2001] (reanalysis), and (b) Western North Pacific (100 – 250 m) (model transect connects through latitude/longitude of each data point): (A) ~6.75‰ at 0°N/S, 140°E [Yoshikawa *et al.*, 2006]; (B) ~6.0‰ at 6°N, 125°E [Kienast *et al.*, 2008]; (C) ~3.0‰ at 25°N, 123°E [Liu *et al.*, 1996].

312

$\delta^{15}\text{NO}_3^-$				<i>Excess P</i>		
<i>Model</i>	<i>r</i>	<i>STD</i>	<i>RMS</i>	<i>r</i>	<i>STD</i>	<i>RMS</i>
CTL	0.668	1.76	1.33	0.520	1.30	1.27
FeLim	0.680	1.33	0.982	0.530	0.898	1.01

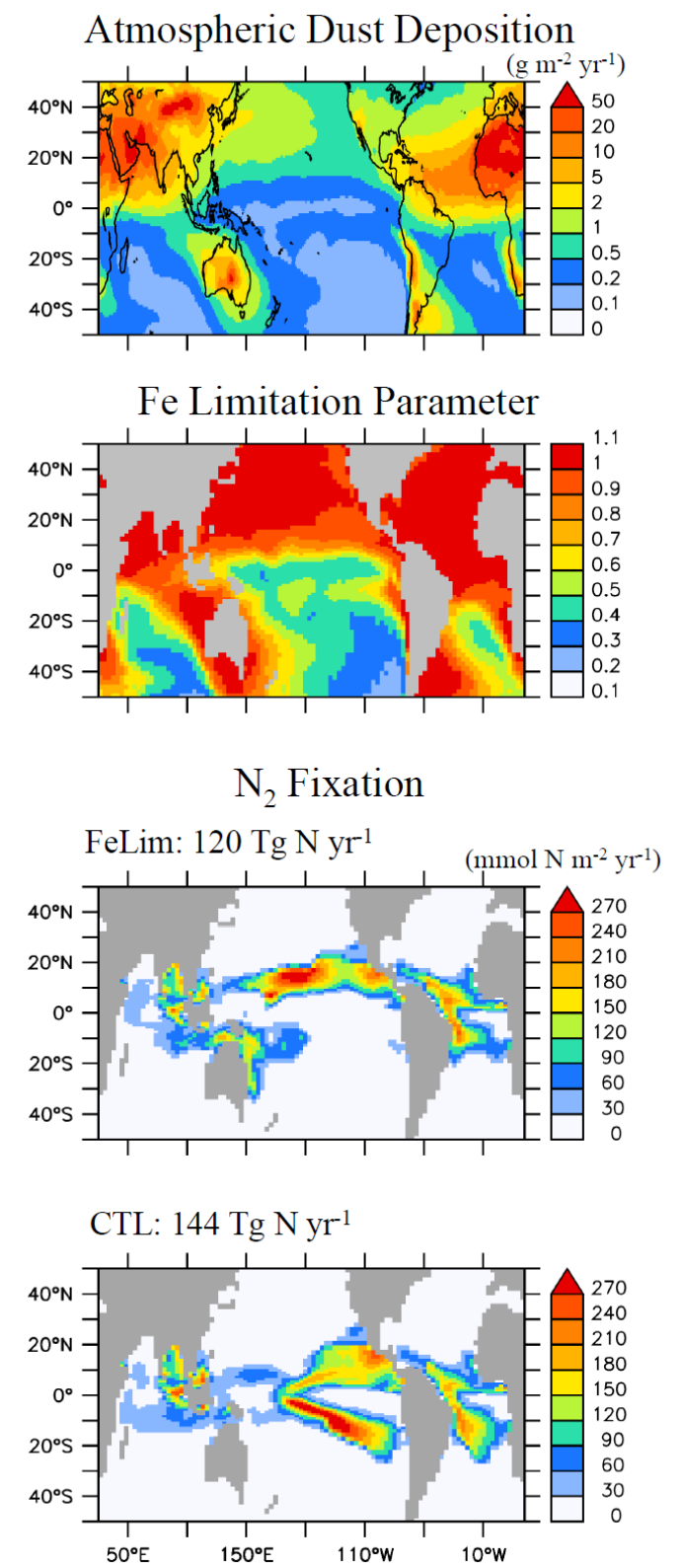
313 **Table 1.** Global measures of $\delta^{15}\text{NO}_3^-$ and xsP model performance: correlation coefficient (r),

314 standard deviation (STD), and root mean squared (RMS) error. STD and RMS have been

315 normalized by the standard deviation from the observations.

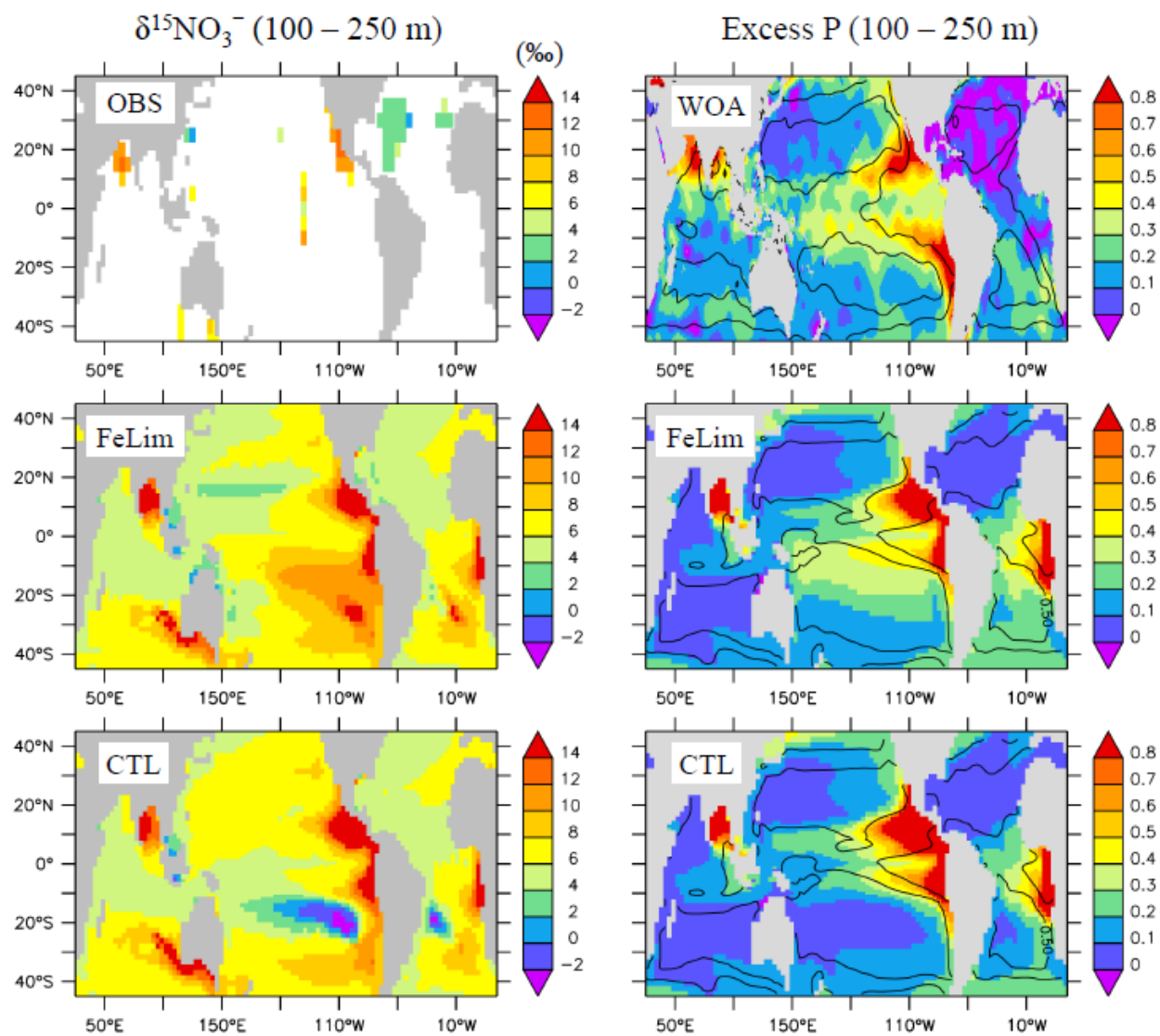
316

Figure 1.



319

Figure 2.



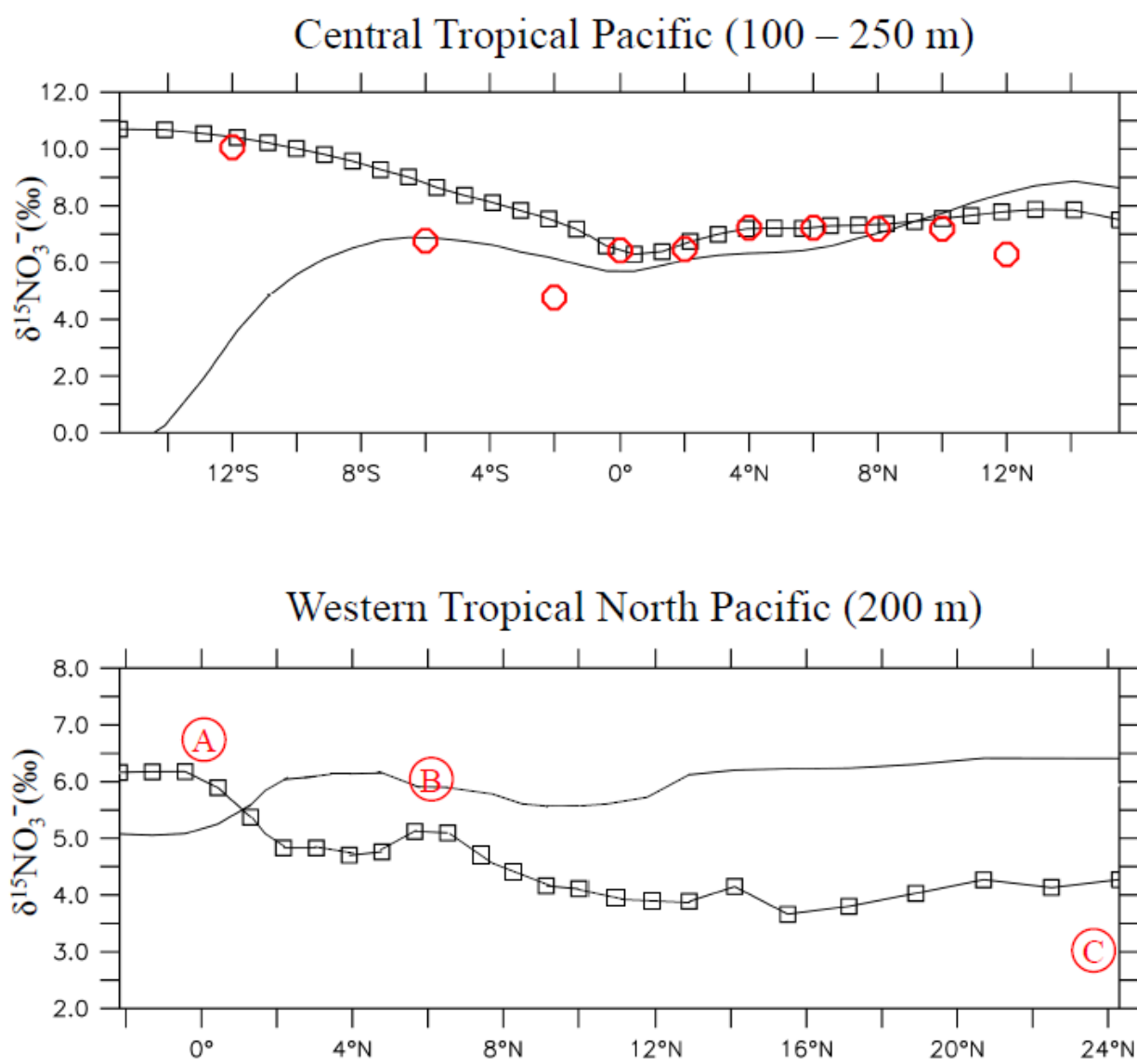
320

321

322

323

Figure 3.



324